

Secretory leakage of IgG1 aggregates from recombinant Chinese hamster ovary cells

Masayoshi Onitsuka,^{1,*} Yukinori Kadoya,² and Takeshi Omasa³

Graduate School of Technology, Industrial and Social Sciences, Tokushima University, 2-1 Minamijosanjima-cho, Tokushima 770-8506, Japan,¹ Graduate School of Advanced Technology and Science, Tokushima University, 2-1 Minamijosanjima-cho, Tokushima 770-8506, Japan,² and Graduate School of Engineering, Osaka University, U1E-801, 2-1 Yamadaoka, Suita, Osaka 565-0871, Japan³

Received 11 September 2018; accepted 30 November 2018
Available online 21 December 2018

Aggregation of therapeutic antibodies is one of the most important issues to be resolved in manufacturing processes because of reduced efficacy and immunogenicity. Despite aggregation studies *in vitro*, little is known about the aggregation mechanism in cell culture processes. In this study, we investigated the process of aggregate formation of IgG1 antibodies during the culture of Chinese hamster ovary (CHO) cells to determine how aggregation occurs. A recombinant CHO cell line was cultivated in a bioreactor, and purified IgG1 from daily culture supernatants was analyzed by size exclusion chromatography. We found a linear correlation between the peak plots of IgG1 by-products, dimeric and aggregated IgG1, and integrated viable cell density, indicating that these by-products were secreted from CHO cells at a constant secretion rate. In addition, aggregate formation was not reproduced in pseudo-culture experiments, and the solution structures of intracellular and extracellular IgG1 aggregates were similar. These results support the concept of secretory leakage of IgG1 by-products. Secreted aggregates appeared to be in an alternatively folded state, which can pass through the protein quality control system in mammalian cells.

© 2018, The Society for Biotechnology, Japan. All rights reserved.

[Key words: Antibody aggregation; Antibody production; Chinese hamster ovary cells; Monoclonal antibody; Protein quality control; Protein secretion]

Monoclonal antibodies (mAbs) are the fastest growing class of biological drugs. The manufacturer of almost all mAbs employs Chinese hamster ovary (CHO) cells as the host cells for production (1). It is well known that recombinant antibodies show chemical and structural heterogeneities such as *N*-glycosylation, charge variants, aggregates, and fragments (2). The degree of these heterogeneities is dependent on each recombinant CHO cell line, fermentation conditions, and medium design. Product quality attributes of therapeutic antibodies should be designed in the manufacturing process owing to quality assurance of therapeutic efficacy, i.e., a quality by design (QbD) concept (3).

Aggregation of therapeutic proteins is involved in potential risks for loss of efficacy and aggregate-induced immunogenicity in patients (4). Antibody aggregation can occur at various stages including the up- and down-stream processes in manufacturing, formulation, and long-term storage (5,6). Aggregates have been characterized in mAb purification and formulation. Low pH elution can induce mAb aggregation in protein A chromatography (7,8). A modified protocol, stepwise elution including arginine, has been proposed to remove aggregates (9). In formulation and long-term storage, the management of colloidal stability of an antibody by buffer design is quite important to reduce aggregation and oligomerization (10,11).

Although much is known about mAb aggregation in purification and formulation, it is less understood how recombinant antibodies aggregate during the cell culture process. Process conditions including bioreactor pH, temperature, dissolved oxygen, and osmolality have significant effects on antibody aggregation in cell culture (2,12,13). In terms of the *N*-glycosylation status of the antibody Fc region, aggregation appears to be induced by aglycosylation and/or deglycosylation in bioprocesses (14,15). However, how aggregation occurs during cell culture are unknown. In some cases, secreted antibody molecules may form aggregations (5), and components in serum-free medium have been reported to affect aggregate formation (12,16,17). Furthermore, studies have reported intracellular aggregation of recombinant proteins (13,18,19). These aggregations were due to improper cleavage of the light chain of IgG1 and its insoluble precipitates in the cellular fraction (18), as well as misassembled heavy chains resulting in intracellular aggregates (19). In addition to these studies, enhanced protein production by cell engineering approaches involving unfolded protein response (UPR) genes and molecular chaperones implies that protein aggregates accumulate in cells (20). Despite these studies, the relationship between intracellular aggregates and the aggregation of recombinant antibodies during cell culture processes is not yet clear. To our knowledge, there is no study on the secretion of intracellular aggregates into cultures of CHO cells. Secretion is less likely to occur because of the protein quality control systems in mammalian cells (21,22). Accumulation of unfolded or misfolded proteins in the endoplasmic reticulum (ER) induces the UPR accompanied by

* Corresponding author. Tel.: +81 88 656 7408.

E-mail address: onitsuka@tokushima-u.ac.jp (M. Onitsuka).

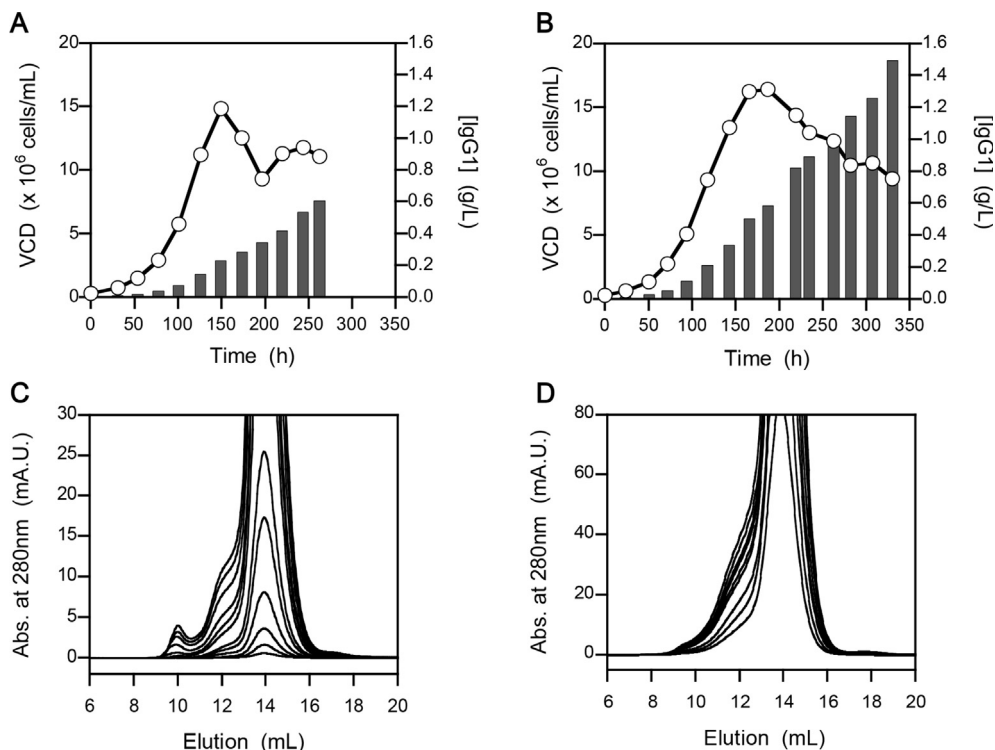


FIG. 1. (A, B) CHO cell culture employing processes A (A) and B (B). Open circles and bars are the viable cell density (VCD, left Y axis) and IgG1 production (right Y axis), respectively. (C) SEC analysis of IgG1 during cell culture in process A. Profiles at days 0–11 are superimposed. (D) SEC analysis in process B. Profiles at days 6–14 are superimposed.

chaperone/foldase expression and translational attenuation, resulting in restored protein homeostasis. Unrestored proteins are finally removed by ER-associated degradation (ERAD).

In this study, we investigated the process of aggregate accumulation of a recombinant antibody in 4 L bioreactor cultures to explore antibody aggregation in the CHO cell culture process. Importantly, our study indicates secretory leakage of intracellular IgG1 aggregates. The secreted aggregate had a misfolded state with a non-native β -strand structure. The specific misfolded conformation of the antibody appeared to be secreted from CHO cells by passing through their protein quality control systems.

MATERIALS AND METHODS

CHO cell culture The CHO-Hcd6 cell line (23) was used in this study. The cell line was cultured in a BCP-07NP3 bioreactor (ABLE Biott, Tokyo, Japan) with a working volume of 4 L serum-free medium Top2 (Irvine scientific, Santa Ana, CA, USA). The cells were inoculated at 0.3×10^6 cells/mL into the culture vessel. Bioreactor settings were as follows: 40% dissolved oxygen by intermittent O_2 flow, 37 °C, pH 7.0, 80 rpm agitation, air flow of 400 mL/min, and CO_2 flow of 20 mL/min. Two types of feeding method, process A and B, were used. In process A, 150 mL feed medium prepared in-house was added at days 4, 6, 8, 9, and 10. In process B, daily feeding was started at day 4. Fifty milliliters and 200 mL of feed medium were added at days 4 and 7, respectively. At other days, 100 mL feed medium was added to the culture. In process B, the feeding method was changed to daily feeding to prevent depletion of glucose and lactate in serum-free medium. Before feeding, 50 mL of culture was sampled from the culture vessel for IgG1 analysis. Viable cell density and cell viability were measured using a Vi-CELL XR (Beckman Coulter, Fullerton, CA, USA).

IgG1 purification and analysis The IgG1 antibody was purified from 40 mL of daily culture samples with a HiTrap rProtein A FF column (GE Healthcare, Buckinghamshire, UK). Purified IgG1 was analyzed by size exclusion chromatography (SEC) with a Superdex 200 column (GE Healthcare). The relative contents of aggregated, dimeric, and monomeric IgG1 were estimated by peak deconvolution analysis using Kaleidagraph software (Synergy Software, Reading, PA). For analysis of intracellular IgG1 polypeptides, 18 g of cell pellet harvested in process B was lysed with 110 mL M-PER Mammalian Protein Extraction Reagent (ThermoFisher Scientific,

Waltham, MA, USA). The lysed solution was dialyzed against PBS and then subjected to affinity purification with a HiTrap rProtein A-HiTrap Protein L (GE Healthcare)-conjugated column. Purified intracellular IgG1 polypeptides were analyzed by SEC with a Superdex 200 column. A gel filtration standard (BioRad, Hercules, CA, USA) was used as the molecular weight marker. In SEC analysis, aggregated and monomeric IgG1 were fractionated and purified. Circular dichroism (CD) spectra were measured using a Jasco J-820 spectropolarimeter (Jasco, Tokyo, Japan). Antibody concentration were diluted to 0.4 mg/mL in TBS buffer (pH 7.4). The concentration of monomeric IgG1 was spectroscopically determined using an excitation coefficient at 280 nm, $E_{1\%}^{1\text{cm}}$ of 14. The concentration of aggregated antibodies was determined with Pierce 660 nm Protein Assay Reagent (ThermoFisher Scientific). Purified monomeric IgG1 was used as the reference standard.

Kinetic analysis of proteins in culture medium Protein concentrations in culture media were analyzed by the following equation:

$$P = \rho \int_{t_1}^{t_2} X dt \tag{1}$$

where P and ρ are protein concentrations determined experimentally and the specific production rate (pg/cell/day), respectively. An integral term is integrated viable cell density (IVCD). IVCD was calculated by the following equation:

$$\int_{t_1}^{t_2} X dt \approx \sum \frac{(t_2 - t_1)(X_2 - X_1)}{2} \tag{2}$$

where t_1 and t_2 are the time of cultivation, and X_1 and X_2 are viable cell densities at time t_1 and t_2 , respectively. IgG1 concentrations in media were measured with an Octet QK system and protein A biosensor (Pall ForteBio, Freont, CA, USA). Monomeric IgG1 was used as the reference standard. CHO host cell protein (HCP) in medium was measured with an EnSpire multi-label reader and CHO HCP broad reactivity AlphaLISA detection kit (PerkinElmer, Waltham, MA, USA).

Pseudo-cultivation experiments In pseudo-cultivation experiments, 11 mg/mL monomeric IgG1 solution was added to serum-free Top2 medium and the culture supernatant of CHO-K1 cells (ATCC CRL-9618), resulting in a final concentration of 1 mg/mL IgG1. Serum-free adapted CHO-K1 cells were cultivated in Top2 medium, and the culture supernatant at a viable cell density of 17.3×10^6 cells/mL (96.9% viability) was centrifuged to remove cells. The finally prepared culture supernatant and TOP2 medium including 1 mg/mL IgG1 were incubated in 125-mL Erlenmeyer flasks (Corning Inc., Corning, NY, USA) at a

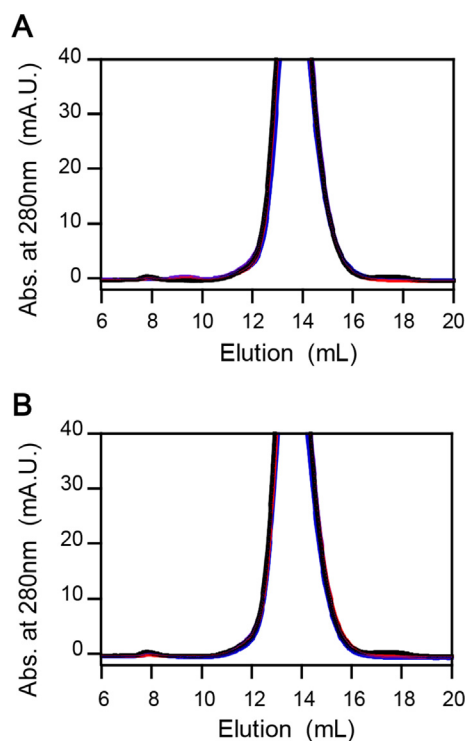


FIG. 2. SEC analysis of the IgG1 antibody in pseudo-cultivation experiments. The IgG1 concentration was 1 mg/mL. (A, B) Overlays of SEC profiles in serum-free medium (A) and the culture supernatant of CHO-K1 cells (B). SEC profiles at day 0 (black), day 7 (red), day 14 (purple), and day 21 (blue) are superimposed. (For interpretation of the references to color in this figure legend, the reader is referred to the Web version of this article.)

working volume of 20 mL at 37 °C with 80% humidity and shaking at 80 rpm in a Climo-shaker ISF1-X (Kuhner, Basel, Switzerland). IgG1 was purified with an Ex-Pure Protein A spin column (Kyoto Monotech, Kyoto, Japan) from 1 mL of culture supernatant and analyzed by SEC with a Superdex 200 column.

RESULTS

Accumulation of aggregated IgG1 in the CHO cell culture process

The CHO cell line producing IgG1 was cultivated by two feeding methods (Fig. 1A,B). Cell cultures were stopped when the cell viability decreased to 75%. Although the maximum viable cell densities were comparable between processes A and B, the difference in feeding method significantly affected the final IgG1 titer. Process B with daily feeding resulted in a high IgG1 titer of 1500 mg/L, whereas that of process A was 600 mg/L. IgG1 was purified from 40 mL of culture supernatant at days 3–11 in process A and days 6–14 in process B, and then purified IgG1 was analyzed by SEC (Fig. 1C,D; the whole elution profiles are shown in Fig. S1). Three oligomeric states were observed in SEC elution profiles. The peaks or shoulders at elution volumes of 9.5–10, 11.5–12, and 13.5–14 mL corresponded to high-order aggregated, dimeric, and monomeric IgG1, respectively. We confirmed that the three fractionated oligomeric IgG1s were composed of IgG1 heavy and light chains by reducing SDS-polyacrylamide gel electrophoresis (PAGE) (Fig. S2A). All peak heights of elution profiles were monotonically increased with cultivation time, indicating that dimeric and aggregated IgG1, by-products of monomeric IgG1, were dynamically increased in the cell culture process. It should be noted that these by-products were not formed in the protein A affinity purification process in which IgG1 was exposed to an acidic solution, but in the cell culture process, because monomeric

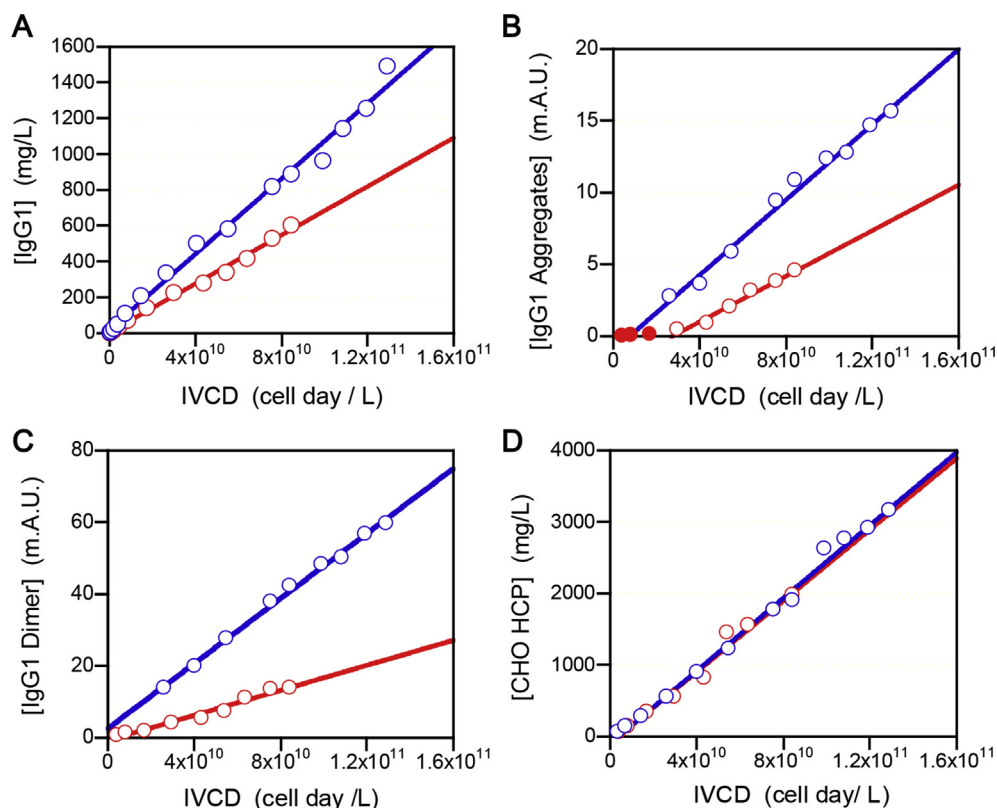


FIG. 3. IVCD plots of IgG1 (A), aggregated antibodies (B), dimeric IgG1 (C), and CHO host cell protein (HCP) (D). Red and blue circles are plots of process A and B, respectively. Lines are the results of linear correlation analysis. (B, C) The plots at days 3–11 in process A and those at days 6–14 in process B are shown. In linear correlation analysis of IgG1 aggregates in process A, the plots at days 3–5 (filled red circles in panel B) were omitted from the analysis because of undetectable peak areas.

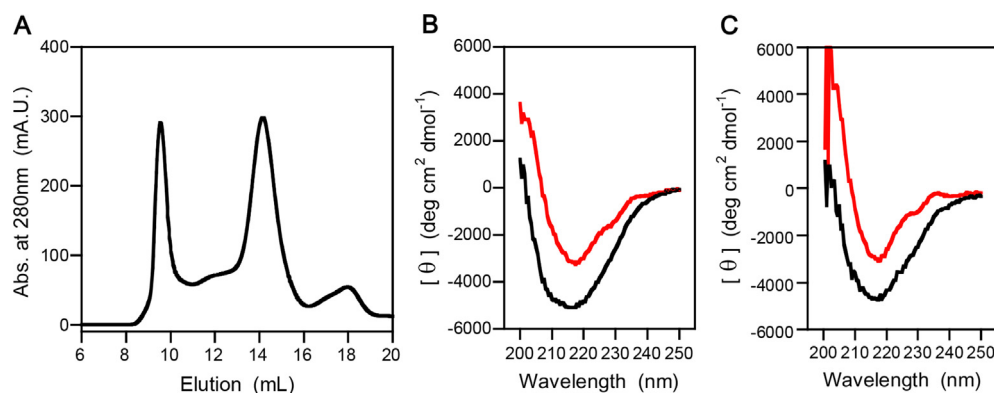


FIG. 4. (A) SEC analysis of intracellular IgG1 and its by-products purified by protein A-L affinity chromatography. (B, C) CD spectra of intracellular (B) and extracellular IgG1 (C). Red and black curves are spectra of monomeric and aggregated IgG1, respectively. (For interpretation of the references to color in this figure legend, the reader is referred to the Web version of this article.)

IgG1 re-purified with a protein A column showed no tendency to aggregate and retained its monomeric form (Fig. S3 and Table S1).

Pseudo-cultivation experiments One plausible explanation for increased IgG1 by-products is that monomeric IgG1 was converted into dimeric and aggregated forms in the culture medium. Stresses including medium pH, temperature, oxidation, and cultivation time may induce IgG1 aggregation during the cell culture process (5,6). Estimating the conversion rate of monomeric IgG1 to by-products would facilitate understanding IgG1 aggregation in cell culture. Pseudo-cultivation experiments, as a simplified model for the estimation, were carried out. Monomeric IgG1 was added to serum-free medium (Fig. 2A) and the culture supernatant of CHO-K1 cells (Fig. 2B), whereby viable cells were excluded from the experiments. We verified that, in the culture supernatant, by-product formation was accelerated by secreted components such as HCPs from CHO-K1 cells. Unexpectedly, all elution profiles at days 7, 14, and 21 were superposed on that at day 0, and we observed no increase in the peak heights of dimeric or aggregated IgG1 (Fig. 2A,B). The accumulation of IgG1 by-products could not be realized in pseudo-cell culture experiments. These results suggest that the monomeric IgG1 was not converted into dimeric or aggregated IgG1 in the cell culture medium.

Kinetic analysis of protein secretion Another possibility for increased IgG1 dimers and aggregates is secretion of these by-products from CHO cells. However, at present, it is quite difficult to directly observe specific secretion of IgG1 dimers and aggregates. To investigate this possibility, we kinetically analyzed the cell culture data combined with the SEC profiles. The basic procedure is the same as that for estimation of the specific production rate (ρ), where the protein concentrations are plotted as a function of IVCD. The specific production rate of IgG1 was calculated by Eq. 1 (Fig. 3A). Plots of both process A and B showed a linear correlation (correlation coefficients: $r = 0.996$ and 0.995 for process A and B, respectively), resulting in ρ of 6.77 and 10.5 (pg/cell/day) for process A and B, respectively. Such linearity indicated that cells in both processes maintained a constant rate of IgG1 secretion during the culture process. The same analysis was applied to IgG1 by-products. Peak areas of aggregated and dimeric IgG1 calculated by peak deconvolution analysis were plotted as a function of IVCD (Fig. 3B,C). Details of peak deconvolution analysis are shown in Figs. S4 and S5 and Table S2. Importantly, during the culture process, the plots of aggregated IgG1 in process B and IgG1 dimers in both processes showed a linear correlation. For IgG1 aggregates in process A, the plots at days 6–11 (open red circle in Fig. 3B) showed linearity. Correlation coefficients (r) were 0.994 and 0.988 for process A and B, respectively (IgG1 aggregates, Fig. 3B), and 0.998 and 0.984 for process A and B, respectively (IgG1 dimers, Fig. 3C). Although the

concentrations of IgG1 aggregates and dimers could not be estimated, the linearity of the plots with high correlation indicated that these by-products were secreted from recombinant CHO cells at a constant secretion rate. The peak area plots and corresponding slope in process B were higher than those in process A, indicating that the cells in process B secreted more by-products than those in process A in accordance with the specific production rate, ρ . CHO HCP was proportional to IVCD with the same slopes in both processes (Fig. 3D), indicating that the protein secretory capacities of CHO cells themselves were unchanged by the feeding methods. The differences in secretion of by-products were probably due to the specific production rates (ρ), i.e., a higher productive process would result in increased aggregated and dimeric IgG1. Furthermore, we calculated the slope ratio of the linear correlation in the IVCD plots: the slopes of IgG1 aggregates and dimers (Fig. 3B,C) were divided by their specific production rates (ρ , Fig. 3A). This calculation clearly showed the concentration dependency of by-product secretion. The calculated index for IgG1 dimer was 2.56×10^{-2} (process A) vs. 4.30×10^{-2} (process B), suggesting that dimer formation was dependent on the concentration of the main product, IgG1 monomer. Because the dimer content was not increased in pseudo-cultivation experiments (Fig. 2), dimer secretion was likely proportional to intracellular IgG1 monomer. On the other hand, the indices for IgG1 aggregates in both processes were nearly identical: 1.17×10^{-2} (process A) vs. 1.24×10^{-2} (process B). The independent formation of aggregated IgG1 seems to be related to the IgG1 folding process in CHO cells, rather than folded IgG1 content.

Analysis of intracellular IgG1 We validated the secretion of IgG1 aggregates and dimers by measuring the accumulation of these by-products in CHO cells. A harvested cell pellet in process B was mildly lysed with non-denaturing protein extraction reagent. The lysed cell solution was dialyzed against PBS, followed by protein A-L affinity chromatography. The SEC profile of the purified solution showed two sharp peaks at elution volumes of 9.5–10 and 14 mL, and two broad bumps at 12 and 18 mL (Fig. 4A). As shown in Fig. 1, the components with elution peaks at 9.5–10, 12, and 14 mL corresponded to aggregated, dimeric and monomeric IgG1, respectively. SDS-PAGE analysis showed that the broad bump at 17–18 mL was a mixture of free light chain and light chain dimers (Fig. S2B). Because aggregate formation was hardly induced by treatment of purified IgG1 monomer with cell lysis buffer or the acidic solution in the affinity purification, the multiple peaks in the SEC profile were indicative of the intracellular oligomeric state of IgG1 polypeptides. Therefore, we confirmed that considerable amounts of IgG1 aggregates had accumulated in recombinant CHO cells. The solution structure of intra- and extra-cellular IgG1 was

examined by CD spectral measurement (Fig. 4B,C). Extracellular IgG1 was purified from culture medium by protein A affinity chromatography and SEC. CD spectra of intra- and extra-cellular IgG1 monomers (red line in Fig. 4B,C) exhibited the typical secondary structure of the IgG1 molecule, showing a large negative band at 218 nm (24,25). The negative band is characteristic of the β -sheet content of the antibody domain. Although a slight difference was observed between intra- and extra-cellular IgG1 monomers, which might have resulted from differences in affinity purification methods (protein A/L vs protein A affinity chromatography), the overall shapes of spectra were similar to each other. Aggregated IgG1 (black line in Fig. 4B,C) showed a significant increase in negative CD intensity at 218 nm, and a change was observed in the spectrum shape. These changes were indicative of the misfolded state consisting of a non-native β -sheet structure that was not formed in monomeric IgG1. Similar to the IgG1 monomer, intra- and extra-cellular aggregates showed a similar overall structure despite a small difference in their CD spectra. These data support the idea that IgG1 by-products, dimeric and aggregated IgG1, were secreted from recombinant CHO cells during the cell culture process.

DISCUSSION

Although aggregation of therapeutic proteins is problematic in bioprocessing (5,6), little is known about aggregations in the cell culture process. The important aspects are how aggregation of recombinant proteins occur during cell culture. In this study, we found secretory leakage of IgG1 aggregates from recombinant CHO cells. Kinetic analysis of bioreactor cultures showed linear correlations between IVCDs and IgG1 by-products (Fig. 3), indicating that IgG1 dimers and aggregates continued to be secreted from CHO cells during culture at a constant secretion rate. This result was supported by pseudo-cell culture experiments and analyses of intracellular IgG1. Aggregate formation could not be realized by addition of monomeric IgG1 to the serum-free medium or culture supernatant of CHO-K1 cells (Fig. 2). Additionally, a considerable amount of aggregated IgG1 had accumulated in CHO cells, and the structure of intracellular IgG1 aggregates resembled that of extra-cellular IgG1 aggregates (Fig. 4). To the best of our knowledge, this is the first study indicating that IgG1 aggregates are secreted from CHO cells in the cell culture process.

Secretory leakage of aggregated IgG1 appears to be inconsistent with the fact that CHO cells produce correctly folded proteins. In mammalian host cells, a quality control system for protein folding exists in the ER. Proper folding is assisted by molecular chaperones expressed in response to accumulation of unfolded or misfolded proteins, the so-called UPR. In addition to chaperone induction, the UPR includes translational attenuation, and ERAD is also induced to avoid unfolded and misfolded protein accumulation in cells. A UPR-based cell engineering approach has contributed to enhanced protein production in CHO cells (26–33). These successful studies indicate that a quality control system including the UPR positively acts in CHO cells. In this study, intracellular IgG1 aggregates, which formed a misfolded structure composed of a non-native β -strand, were secreted from CHO cells. High transcriptional and translational levels can induce accumulation of misfolded and aggregated antibodies by overloading the protein-folding capacity in the ER. In recombinant cells, intracellular aggregates of IgGs have been reported to be stored in the ER as Russel bodies (RBs) (34). The formation of RBs depends on the physicochemical properties of recombinant antibodies. IgGs with high condensation/aggregation propensities are prone to form RBs in the ER (35). Bottlenecks in antibody biosynthesis can lead to intracellular aggregation and inefficient secretion (13,18,19). Aggregated proteins are a

heterogeneous mix of states in terms of conformation, molecular weight/size, and reversibility (36,37). Some states can be stored in the ER as RBs, while others can result in secretory leakage. Alternatively folded states (AFSs) of antibodies are reported to be induced by physicochemical stresses (38,39). Misfolded aggregates observed in this study can be considered as a naturally occurring AFS, and the AFS may not be trapped by the UPR, ERAD, or RB formation, resulting in protein secretion. Accordingly, we hypothesize that, in recombinant CHO cells, some misfolded and aggregated states of antibodies, in addition to dimeric antibodies and monomeric IgG1, can pass through protein quality control systems.

Based on QbD concept, process optimization and design of experiments approaches have been employed to reduce aggregation in cell culture (40,41). A medium supplementation approach using dimethyl sulfoxide, glycerol, and polysorbate-80 is useful for less aggregate formation by increasing protein stability (42,43). Our previous report showed suppression of antibody aggregation by trehalose supplementation (44). Trehalose appears to prevent the polymerization steps in aggregate growth. In an effort to develop a cell culture process for less aggregation, direct monitoring of aggregated antibodies is valuable to evaluate whether the tested approach is useful. Recently, Watanabe et al. (45,46) and Senga et al. (47) have reported the artificial protein AF.2A1 that specifically recognizes non-native IgG (45–47). Probe-based monitoring of aggregated antibodies will be applicable to process development as a process analytical technology. In addition, AF.2A1 may be useful to investigate the secretory process of aggregated antibodies by immunostaining.

In this study, we showed that IgG1 by-products, aggregated and dimeric IgG1, were secreted from recombinant CHO cells, in addition to monomeric IgG1. Structural characterization of secreted and intracellular aggregates of antibodies combined with mutation analysis would be valuable to test our hypothesis of passing through the protein quality control system and investigate the secretory mechanism of misfolded antibody aggregates.

Supplementary data to this article can be found online at <https://doi.org/10.1016/j.jbiosc.2018.11.015>.

ACKNOWLEDGMENTS

This research was supported by Japan Agency for Medical Research and Development (AMED) under Grant Number JP17ae0101003. The authors thank Dr. Aya Kobayashi and Ms. Maiko Togawa (Manufacturing Technology Association of Biologics; MAB) for technical assistance in cell culture experiments. We also thank Mitchell Arico from Edanz Group for editing a draft of this manuscript. The authors declare no financial or commercial conflict of interest.

References

1. Kunert, R. and Reinhart, D.: Advances in recombinant antibody manufacturing, *Appl. Microbiol. Biotechnol.*, **100**, 3451–3461 (2016).
2. Bruhlmann, D., Jordan, M., Hemberger, J., Sauer, M., Stettler, M., and Broly, H.: Tailoring recombinant protein quality by rational media design, *Biotechnol. Prog.*, **31**, 615–629 (2015).
3. Craven, S. and Whelan, J.: Process analytical technology and quality-by-design for animal cell culture, pp. 647–688, in: Al-Rubeai, M. (Ed.), *Animal cell culture*. Springer, Cham (2015).
4. Felipe, V., Hawe, A., Schellekens, H., and Jiskoot, W.: Aggregation and immunogenicity of therapeutic proteins, pp. 403–433, in: Wang, W. and Roberts, C. J. (Eds.), *Aggregation of therapeutic proteins*. John Wiley & Sons, Inc., Hoboken, NJ (2010).
5. Cromwell, M. E., Hilario, E., and Jacobson, F.: Protein aggregation and bioprocessing, *AAPS J.*, **8**, E572–E579 (2006).
6. Vazquez-Rey, M. and Lang, D. A.: Aggregates in monoclonal antibody manufacturing processes, *Biotechnol. Bioeng.*, **108**, 1494–1508 (2011).

7. **Shukla, A. A., Gupta, P., and Han, X.:** Protein aggregation kinetics during protein A chromatography. Case study for an Fc fusion protein, *J. Chromatogr. A*, **1171**, 22–28 (2007).
8. **Joshi, V., Shivach, T., Kumar, V., Yadav, N., and Rathore, A.:** Avoiding antibody aggregation during processing: establishing hold times, *Biotechnol. J.*, **9**, 1195–1205 (2014).
9. **Yada, T., Nonaka, K., Yabuta, M., Yoshimoto, N., and Yamamoto, S.:** Choosing the right protein A affinity chromatography media can remove aggregates efficiently, *Biotechnol. J.*, **12**, 1600427 (2017).
10. **Uchiyama, S.:** Liquid formulation for antibody drugs, *Biochim. Biophys. Acta*, **1844**, 2041–2052 (2014).
11. **Nicoud, L., Owczarz, M., Arosio, P., and Morbidelli, M.:** A multiscale view of therapeutic protein aggregation: a colloid science perspective, *Biotechnol. J.*, **10**, 367–378 (2015).
12. **Jing, Y., Borys, M., Nayak, S., Egan, S., Qian, Y., Pan, S. H., and Li, Z. J.:** Identification of cell culture conditions to control protein aggregation of IgG fusion proteins expressed in Chinese hamster ovary cells, *Process Biochem.*, **47**, 69–75 (2012).
13. **Zhou, Y., Raju, R., Alves, C., and Gilbert, A.:** Debottlenecking protein secretion and reducing protein aggregation in the cellular host, *Curr. Opin. Biotechnol.*, **53**, 151–157 (2018).
14. **Kayser, V., Chennamsetty, N., Voynov, V., Forrer, K., Helk, B., and Trout, B. L.:** Glycosylation influences on the aggregation propensity of therapeutic monoclonal antibodies, *Biotechnol. J.*, **6**, 38–44 (2011).
15. **Onitsuka, M., Kawaguchi, A., Asano, R., Kumagai, I., Honda, K., Ohtake, H., and Omasa, T.:** Glycosylation analysis of an aggregated antibody produced by Chinese hamster ovary cells in bioreactor culture, *J. Biosci. Bioeng.*, **117**, 639–644 (2014).
16. **Dengl, S., Wehmer, M., Hesse, F., Lipsmeier, F., Popp, O., and Lang, K.:** Aggregation and chemical modification of monoclonal antibodies under upstream processing conditions, *Pharm. Res.*, **30**, 1380–1399 (2013).
17. **Purdie, J. L., Kowle, R. L., Langland, A. L., Patel, C. N., Ouyang, A., and Olson, D. J.:** Cell culture media impact on drug product solution stability, *Biotechnol. Prog.*, **32**, 998–1008 (2016).
18. **Le, Fourn V., Girod, P. A., Buceta, M., Regamey, A., and Mermod, N.:** CHO cell engineering to prevent polypeptide aggregation and improve therapeutic protein secretion, *Metab. Eng.*, **21**, 91–102 (2014).
19. **Reinhart, D., Sommeregger, W., Debreczeny, M., Gludovacz, E., and Kunert, R.:** In search of expression bottlenecks in recombinant CHO cell lines—a case study, *Appl. Microbiol. Biotechnol.*, **98**, 5959–5965 (2014).
20. **Johari, Y. B., Estes, S. D., Alves, C. S., Sinacore, M. S., and James, D. C.:** Integrated cell and process engineering for improved transient production of a “difficult-to-express” fusion protein by CHO cells, *Biotechnol. Bioeng.*, **112**, 2527–2542 (2015).
21. **Walter, P. and Ron, D.:** The unfolded protein response: from stress pathway to homeostatic regulation, *Science*, **334**, 1081–1086 (2011).
22. **Hetz, C.:** The unfolded protein response: controlling cell fate decisions under ER stress and beyond, *Nat. Rev. Mol. Cell Biol.*, **13**, 89–102 (2012).
23. **Onitsuka, M. and Omasa, T.:** Rapid evaluation of *N*-glycosylation status of antibodies with chemiluminescent lectin-binding assay, *J. Biosci. Bioeng.*, **120**, 107–110 (2015).
24. **Li, C. H., Nguyen, X., Narhi, L., Chemmalil, L., Towers, E., Muzammil, S., Gabrielson, J., and Jiang, Y.:** Applications of circular dichroism (CD) for structural analysis of proteins: qualification of near- and far-UV CD for protein higher order structural analysis, *J. Pharm. Sci.*, **100**, 4642–4654 (2011).
25. **Arosio, P., Rima, S., and Morbidelli, M.:** Aggregation mechanism of an IgG2 and two IgG1 monoclonal antibodies at low pH: from oligomers to larger aggregates, *Pharm. Res.*, **30**, 641–654 (2013).
26. **Tigges, M. and Fussenegger, M.:** Xbp1-based engineering of secretory capacity enhances the productivity of Chinese hamster ovary cells, *Metab. Eng.*, **8**, 264–272 (2006).
27. **Becker, E., Florin, L., Pfizenmaier, K., and Kaufmann, H.:** An XBP-1 dependent bottle-neck in production of IgG subtype antibodies in chemically defined serum-free Chinese hamster ovary (CHO) fed-batch processes, *J. Biotechnol.*, **135**, 217–223 (2008).
28. **Ohya, T., Hayashi, T., Kiyama, E., Nishii, H., Miki, H., Kobayashi, K., Honda, K., Omasa, T., and Ohtake, H.:** Improved production of recombinant human antithrombin III in Chinese hamster ovary cells by ATF4 overexpression, *Biotechnol. Bioeng.*, **100**, 317–324 (2008).
29. **Khan, S. U. and Schroder, M.:** Engineering of chaperone systems and of the unfolded protein response, *Cytotechnology*, **57**, 207–231 (2008).
30. **Omasa, T., Takami, T., Ohya, T., Kiyama, E., Hayashi, T., Nishii, H., Miki, H., Kobayashi, K., Honda, K., and Ohtake, H.:** Overexpression of GADD34 enhances production of recombinant human antithrombin III in Chinese hamster ovary cells, *J. Biosci. Bioeng.*, **106**, 568–573 (2008).
31. **Haredy, A. M., Nishizawa, A., Honda, K., Ohya, T., Ohtake, H., and Omasa, T.:** Improved antibody production in Chinese hamster ovary cells by ATF4 overexpression, *Cytotechnology*, **65**, 993–1002 (2013).
32. **Hussain, H., Maldonado-Agurto, R., and Dickson, A. J.:** The endoplasmic reticulum and unfolded protein response in the control of mammalian recombinant protein production, *Biotechnol. Lett.*, **36**, 1581–1593 (2014).
33. **Onitsuka, M., Kinoshita, Y., Nishizawa, A., Tsutsui, T., and Omasa, T.:** Enhanced IgG1 production by overexpression of nuclear factor kappa B inhibitor zeta (NFKBIZ) in Chinese hamster ovary cells, *Cytotechnology*, **70**, 675–685 (2018).
34. **Stoops, J., Byrd, S., and Hasegawa, H.:** Russell body inducing threshold depends on the variable domain sequences of individual human IgG clones and the cellular protein homeostasis, *Biochim. Biophys. Acta*, **1823**, 1643–1657 (2012).
35. **Hasegawa, H., Woods, C. E., Kinderman, F., He, F., and Lim, A. C.:** Russell body phenotype is preferentially induced by IgG mAb clones with high intrinsic condensation propensity: relations between the biosynthetic events in the ER and solution behaviors in vitro, *MAbs*, **6**, 1518–1532 (2014).
36. **Mahler, H. C., Friess, W., Grauschopf, U., and Kiese, S.:** Protein aggregation: pathways, induction factors and analysis, *J. Pharm. Sci.*, **98**, 2909–2934 (2009).
37. **Sharma, V. K. and Kalonia, D. S.:** Experimental detection and characterization of protein aggregates, pp. 205–256, in: Wang, W. and Roberts, C. J. (Eds.), *Aggregation of therapeutic proteins*. John Wiley & Sons, Inc., Hoboken, NJ (2010).
38. **Feige, M. J., Simpson, E. R., Herold, E. M., Bepperling, A., Heger, K., and Buchner, J.:** Dissecting the alternatively folded state of the antibody Fab fragment, *J. Mol. Biol.*, **399**, 719–730 (2010).
39. **Kannert, D., Brorsson, A. C., Jonsson, B. H., and Enander, K.:** Thermal induction of an alternatively folded state in human IgG-Fc, *Biochemistry*, **50**, 981–988 (2011).
40. **Paul, A. J., Handrick, R., Ebert, S., and Hesse, F.:** Identification of process conditions influencing protein aggregation in Chinese hamster ovary cell culture, *Biotechnol. Bioeng.*, **115**, 1173–1185 (2018).
41. **Handlogten, M. W., Lee-O'Brien, A., Roy, G., Levitskaya, S. V., Venkat, R., Singh, S., and Ahuja, S.:** Intracellular response to process optimization and impact on productivity and product aggregates for a high-titer CHO cell process, *Biotechnol. Bioeng.*, **115**, 126–138 (2018).
42. **Rodriguez, J., Spearman, M., Huzel, N., and Butler, M.:** Enhanced production of monomeric interferon-beta by CHO cells through the control of culture conditions, *Biotechnol. Prog.*, **21**, 22–30 (2005).
43. **Hossler, P., McDermott, S., Racicot, C., and Fann, J. C.:** Improvement of mammalian cell culture performance through surfactant enabled concentrated feed media, *Biotechnol. Prog.*, **29**, 1023–1033 (2013).
44. **Onitsuka, M., Tatsuzawa, M., Asano, R., Kumagai, I., Shirai, A., Maseda, H., and Omasa, T.:** Trehalose suppresses antibody aggregation during the culture of Chinese hamster ovary cells, *J. Biosci. Bioeng.*, **117**, 632–638 (2014).
45. **Watanabe, H., Yamasaki, K., and Honda, S.:** Tracing primordial protein evolution through structurally guided stepwise segment elongation, *J. Biol. Chem.*, **289**, 3394–3404 (2014).
46. **Watanabe, H., Yageta, S., Imamura, H., and Honda, S.:** Biosensing probe for quality control monitoring of the structural integrity of therapeutic antibodies, *Anal. Chem.*, **88**, 10095–10101 (2016).
47. **Senga, Y., Imamura, H., Miyafusa, T., Watanabe, H., and Honda, S.:** AlphaScreen-based homogeneous assay using a pair of 25-residue artificial proteins for high-throughput analysis of non-native IgG, *Sci. Rep.*, **7**, 12466 (2017).